

Fabrication of SnO₂/Zn Core-shell Nanowires and Photoluminescence Properties

Myung Ho Kong^a, Yong Jung Kwon^b, Hong Yeon Cho^b, and Hyoun Woo Kim^{b*}

^a*Industrial Technology Support Division, Korea Institute of Materials Science, Changwon 642-831*

^b*Division of Materials Science and Engineering, Hanyang University, Seoul 133-791*

(Received September 24, 2014, Revised September 29, 2014, Accepted September 30, 2014)

We have fabricated SnO₂/Zn core-shell nanowires by employing a sputtering technique with a Zn target. Scanning electron microscopy indicated that the surface of the nanowires became rougher by the coating. X-ray diffraction of the coated nanowires exhibited the hexagonal Zn diffraction peaks. TEM image of coated structures showed that shell layer was mainly comprised of hexagonal Zn phase. EDX spectra suggested that the shell layer consisted of Zn elements. The photoluminescence spectrum of the coated nanowires in conjunction with Gaussian fitting analysis revealed that the emission was deconvoluted with three Gaussian functions, which are centered at 2.1 eV in the yellow region, 2.4 eV in the green region, and 3.3 eV in the ultraviolet region. We speculated the possible mechanisms of these emission peaks.

Keywords : SnO₂ nanowires, Zn shell, Photoluminescence

I. Introduction

In recent years, one-dimensional (1D) nanometer-scale structures attract great interests, because they contribute to the development of basic sciences and to potential technological applications [1–3]. In particular, the coaxial 1D nanostructures can obtain the peculiar and useful characteristics by the combination of different properties of both core nanowires and shells with different structure, crystallinity, and chemical compositions [4]. Therefore, it has been revealed that they have promising potential applications in future nanodevices, including coaxial-gated transistors and laser diodes [5–7].

Tin oxide (SnO₂) is a direct, wide bandgap (3.6 eV)

n-type semiconductor, having high electrical conductivity, special surface properties, optical transparency, and sensitivity to adsorbed molecules [8,9]. SnO₂ nanowires have a dimensional compatibility with nanoelectronics and high-enough specific surface area. In addition, appropriated doping will easily enhance the electronic and optical properties of SnO₂ nanowires [10–12]. Furthermore, SnO₂ possesses a ferromagnetism at room temperature, by means of the incorporation of various magnetic impurities [13–15].

Accordingly, they have been studied for their use in field-effect transistors [16], transparent devices [17], lithium ion batteries [18], dye-sensitized solar cells [19], spintronics [20], and gas sensors [21,22].

* [E-mail] hyounwoo@hanyang.ac.kr

In the present work, we have coated the core SnO₂ nanowires with Zn shell layers. In the previous paper, Chen et al. reported the fabrication of Zn nanotube arrays, by the electrochemical deposition through nanoporous anodic alumina membranes (AAM) [23]. By comparing with the complicated AAM technique, we have simply formed the Zn nanotube shells on the core nanowires by the direct sputter deposition.

In particular, we have created a composite structure, consisting of SnO₂ nanowire core and Zn nanotube shell. Up to the present, there has been rare report on the formation and characterization of SnO₂/Zn heterointerface. However, there have been numerous papers reporting the effect of Zn doping into SnO₂ structures. The doping of Zn changes or enhances a variety of important materials properties, including gas sensing [24], room-temperature ferromagnetism [25], electrical conductivity [26], photocatalytic performance [27], charge collection efficiency/mobility [28], and thermoelectric properties [29]. Accordingly, the Zn-shelled SnO₂ nanowires prepared in the present work will attract enormous interests in both science and engineering community.

Herein, the formation of uniform shell layer was achieved by the simple sputtering method. Due to its simplicity and well-controllability, this will be considerably applied in the current and future ultra-large-scaled-integration fabrication. We investigated the samples in terms of their structural and photoluminescence (PL) characteristics.

II. Experimental

We carried out the preparation of the core-shell structures by a two-step process. In the first step, we fabricated core SnO₂ nanowires by evaporating the tin (Sn) nano-powder as the source material, in a tube furnace. More detailed procedures for preparing the SnO₂ nanowires were previously outlined [30]. We

have set the substrate temperature to 920°C for 20 min to heat the 3-nm-thick Au-coated Si substrate, under a constant flow of carrier gas consisting of 97% Ar and 3% O₂ with a total pressure of 2 Torr.

In the following step, the substrates were moved to the DC turbo sputter coater (Emitech K575X, Emitech Ltd., Ashford, Kent, UK) for coating the and the Zn shell layers, being similar to a process used in our previous work [31]. At room temperature, the base pressure was set to 2×10^{-4} Pa by using a turbomolecular pump backed by a rotary pump. The deposition was performed for 2 min, with the DC current being kept at 65 mA. This sputtering technique is simple and low-cost process. Upon further development, it will be possible to achieve the very uniform and precise shell coating.

The product were analyzed by X-ray diffraction (XRD) (Philips X'pert MRD diffractometer with CuK α irradiation), field emission scanning electron microscopy (FE-SEM) (Hitachi, S-4200), and transmission electron microscopy (TEM) (Philips, CM-200) with an energy dispersive X-ray spectroscopy (EDX) being installed. The glancing angle (0.5°) technique was employed in the XRD experiments. Photoluminescence spectroscopy (PL) was carried out at room temperature with the 325 nm line from a He-Cd laser (Kimon, 1K, Japan).

III. Results and Discussion

Fig. 1(a) shows an XRD spectrum of pristine SnO₂ nanowires, exhibiting the diffraction peaks of the tetragonal structure of SnO₂ (JCPDS File No. 41-1445). By the way, Fig. 1(b) shows an XRD spectrum of Zn-coated SnO₂ nanowires. It exhibits the very weak diffraction peaks with respect to the hexagonal Zn structure with lattice constants of $a=0.2665$ and $c=0.4947$ nm (JCPDS File No. 04-0831), in addition to the SnO₂-related peaks.

Figs. 2(a) and 2(b) show the SEM images of pristine and Zn-coated SnO₂ nanowires, respectively. While the nanowires maintain the 1D morphology in spite of sputter-coating, it is note worthy that the surface becomes rougher by the coating.

Fig. 3(a) shows a low-magnification TEM image, indicating its straight-line morphology. Fig. 3(b) is an enlarged one, exhibiting a relatively rough surface. A lattice-resolved image on the surface of the nanowire is shown in Fig. 3(c). In the inner region, the distance between the parallel fringes is approximately 0.24 nm, coinciding with to the (200) lattice plane of the tetragonal structure of SnO₂. On the other hand, in the sheath (outer) region, the distance between the neighboring fringes is approximately 0.25 nm, corresponding to the (002) lattice plane of the hexagonal structure of Zn. Fig. 3(d) gives the associated selected area electron diffraction (SAED) pattern, taken along the [0 diffraction spots 2] zone axis. There exist corresponding to the (100), (021), and (121) lattice planes of tetragonal SnO₂. In

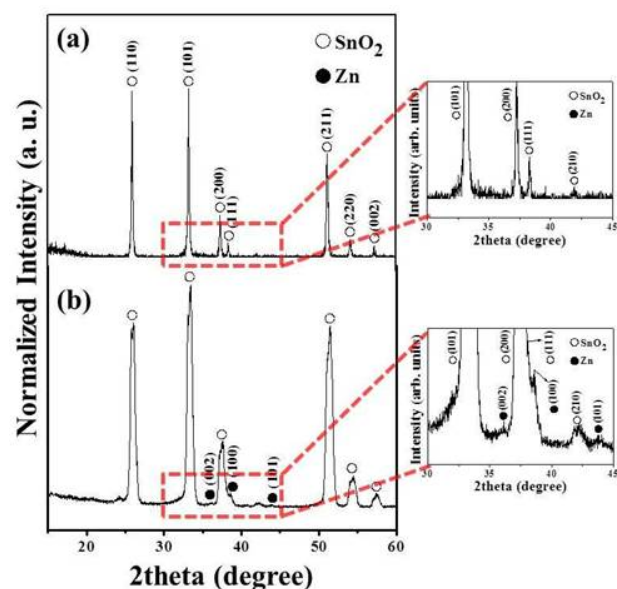


Figure 1. XRD spectra of (a) pristine SnO₂ nanowires and (b) Zn-coated SnO₂ nanowires.

addition, there exist diffraction rings, which are associated with the {002}, {102} and {110} lattice planes of hexagonal Zn. Accordingly, we reveal that the Zn

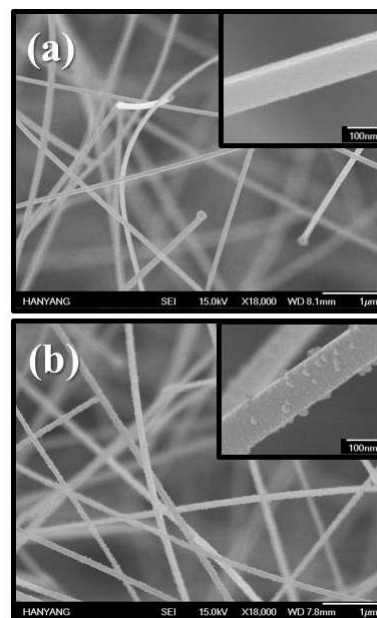


Figure 2. SEM images of (a) pristine SnO₂ nanowires and (b) Zn-coated SnO₂ nanowires (Insets: Enlarged images).

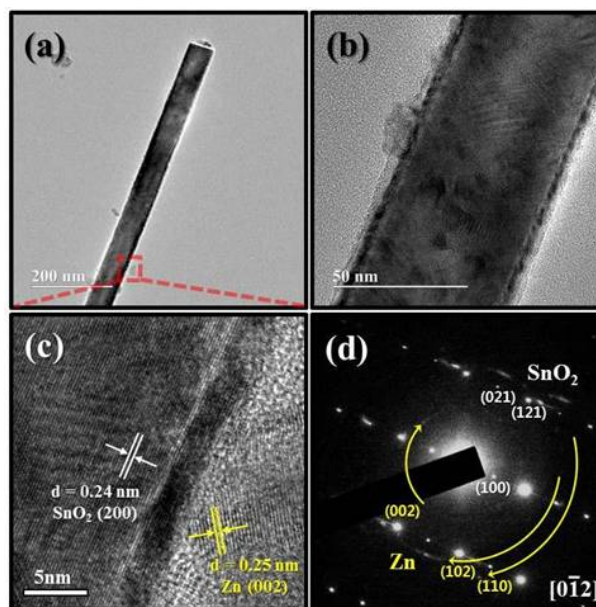


Figure 3. (a) Low-magnification TEM image and (b) enlarged TEM image of a Zn-coated nanowire. (c) High-resolution TEM image near the surface, enlarging the squared region in (a). (d) Corresponding SAED pattern.

shell layer is poly-crystalline, whereas SnO₂ core nanowires are single-crystalline.

In Figs. 4 and 5, we have shown the TEM-EDX results. Elemental maps of Sn, Zn, and O indicate that the coated nanowires are comprised of Sn, Zn, O elements (Fig. 4). In Fig. 5, we carried out the line scan along the diameter of the nanowire. The line scan profiles of Sn and O elements are bell-shaped, confirming the presence of SnO₂ core nanowires. On the other hand, the line scan profile of Zn element is valley-like, suggesting that the Zn atoms mainly reside on the shell part of the nanowire. Accordingly, TEM-EDX analysis is well coincides with the TEM, SEM, and XRD results.

Although there is some surface roughness, SEM and TEM analyses coincidentally indicate that two-dimensional (2D)-growth-mode has been achieved successfully, in spite of the room-temperature sputtering. We surmise that not only the process has been operated with sufficiently low deposition rate but also the SnO₂ surface is crystallographically uni-

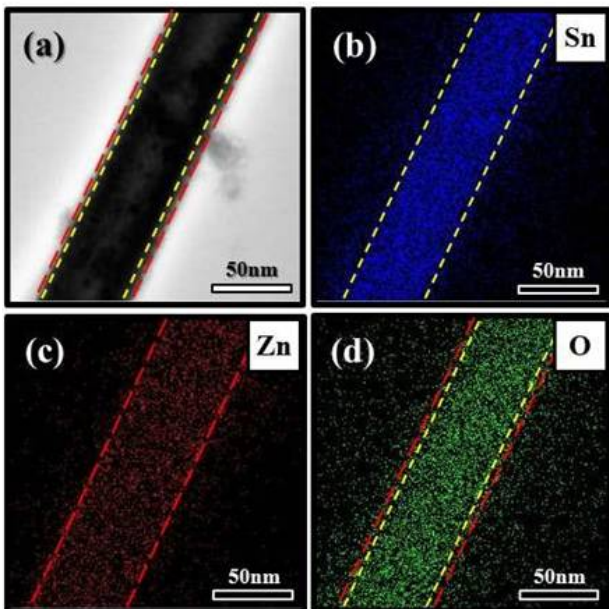


Figure 4. (a) Typical TEM image and corresponding elemental maps of (b) Sn, (c) Zn, and (d) O elements.

form due to its single-crystalline nature.

Fig. 6 shows the PL spectrum of the coated SnO₂ nanowires, being measured at 300K. Gaussian fitting analysis indicated that the best fit of the emission was obtained with three Gaussian functions, which are centered at 2.1 eV in the yellow region, 2.4 eV in the green region, and 3.3 eV in the violet region, respectively. The excitation energy of the He-Cd laser is 3.82 eV, which overcomes the energy band gap of SnO₂ (3.6 eV) [32]. It is well known that the yellow emission from SnO₂ structure is originated from O vacancies or Sn interstitials [33,34]. Also, Jeong et al. observed the green emission peak from SnO₂ thin films, revealing the 2.4 eV-centered green emission is closely connected with the oxygen vacancies in the SnO₂ lattice [35].

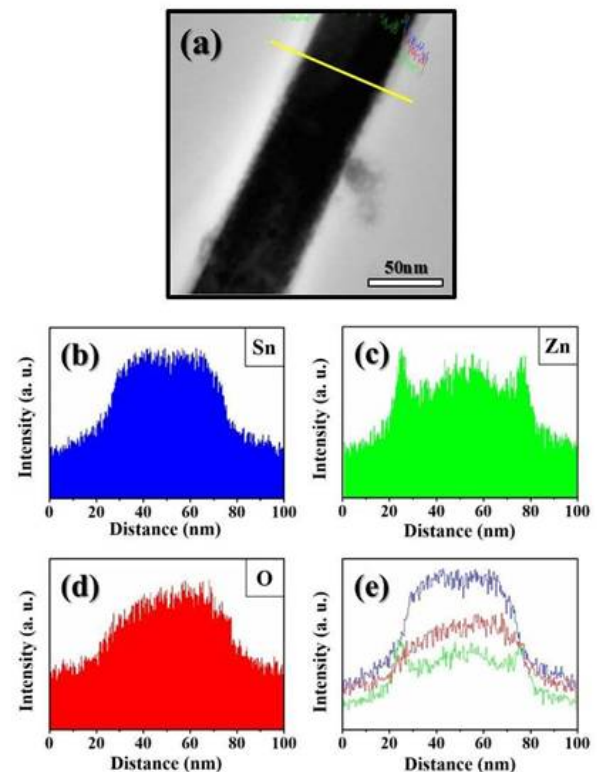


Figure 5. (a) Typical TEM image and corresponding line scans along the diameter of the nanowire with respect to (b) Sn, (c) Zn, and (d) O elements. (e) Line scans overlapping Sn, Zn, and O elements.

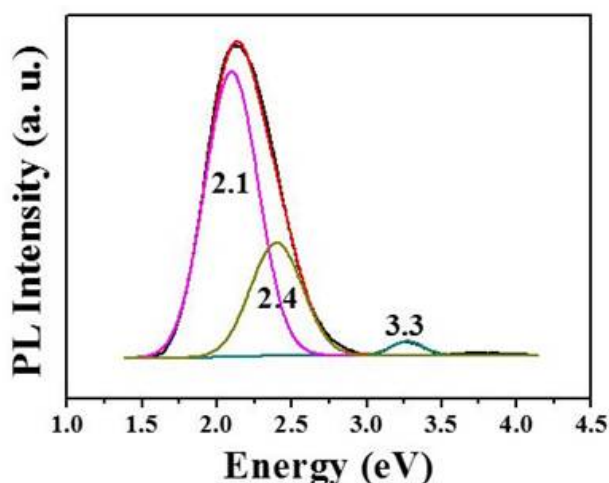


Figure 6. PL spectrum of Zn-coated SnO₂ nanowires. It exhibits the three-peak Gaussian fitting.

We speculated the responsible mechanism for the emission of UV light in Zn-coated SnO₂ nanowires. One possibility is that 3.3 eV-centered peak in the UV region is ascribed to the ZnO structure. Although we could not find out the hexagonal ZnO structure in terms of the XRD and TEM analyses, we surmise that the surface of Zn shell has been partly oxidized, generating the thin ZnO layer. By the way, the sputtering process has been carried out at room temperature and the samples were kept at room temperature afterwards. Accordingly, with the Zn surface being exposed to atmosphere, it is surmised that a layer of atomic oxygen has been adsorbed on the Zn surface [36]. Subsequently, Zn ions diffuse through the oxide layer to the oxide-gas interface, helping in further thickening the ZnO layer. Cabrera and Mott propose the similar mechanism with respect to the oxidation of metals at low temperature [37]. Also, it was revealed that the surface of the smaller Zn nanoparticles can be efficiently transformed to ZnO layer even at low-temperature process [38]. Therefore, we suggest that ZnO shell with its thickness in the nanometer range, in the present study, can be oxidized at room temperature, resulting in the emission of UV light.

The other possibility is related to the defects in the SnO₂ structure. It was reported that Zn-doped SnO₂ nanoparticles exhibited a UV emission [39]. Since the UV emission can be associated with defect energy levels in SnO₂, we surmise that the incorporation of Zn atoms into SnO₂ lattice will generate additional defects, contributing to the emission of UV light.

IV. Conclusion

In summary, we reported the first fabrication of SnO₂/Zn core-shell nanowires. The Zn shell layer was directly coated on SnO₂ nanowires by means of a sputtering technique, in which Zn was used as a sputtering target. We have characterized samples by XRD, SEM, TEM and PL. The surface of the nanowires became rougher by the coating. The shell of the coated nanowires is revealed to be mainly comprised of hexagonal Zn structure. Gaussian fitting analysis indicates that the PL spectrum of coated nanowires is comprised of three emission peaks, centering at 2.1, 2.4, and 3.3 eV, respectively. The 2.1 eV- and 2.4 eV-centered peaks are attributed to O vacancies or Sn interstitials in the SnO₂ lattice. The 3.3 eV peak is regarded to be originated from the defects of ZnO structure, as well as of the SnO₂ structure.

Acknowledgements

This research was supported by Basic Science Research Program through the National Research Foundation of Korea (NRF) funded by the Ministry of Education, Science and Technology (2011-0009946).

References

- [1] A. P. Alivisatos, *Science* **271**, 933 (1996).

- [2] X. Duan, Y. Huang, Y. Cui, J. Wang and C. M. Lieber, *Nature*. **409**, 66 (2001).
- [3] W. A. de Heer, A. Chatelain, and D. Ugarte, *Science*. **270**, 1179 (1995).
- [4] A. M. Morales and C. M. Lieber, *Science*. **279**, 208 (1998).
- [5] Y. Yu, J. Xiang, C. Yang, W. Lu, and C. M. Lieber, *Nature*. **450**, 61 (2004).
- [6] L. J. Lauhon, M. S. Gudixsen, D. Wang, and C. M. Lieber, *Nature*. **420**, 57 (2002).
- [7] H.-J. Choi, J. C. Johnson, R. He, S.-K. Lee, F. Kim, P. Pauzauskie, J. Golberger, R. J. Saykally, and P. Yang, *J. Phys. Chem. B* **107**, 8721 (2003).
- [8] X. Wang, N. Aroonyadet, Y. Zhang, M. Mecklenburg, X. Fang, H. Chen, E. Goo, and C. Zhou, *Nano Lett.* **14**, 3014 (2014).
- [9] P. Camagni, G. Fagila, P. Galinotto, C. Perego, G. Samoggia, and G. Sberveglieri, *Sens. Actuators. B* **31**, 99 (1996).
- [10] A. B. Bhise, D. J. Late, B. Sathe, M. A. More, I. S. Mulla, V. K. Pillai, and D. S. Joag, *J. Exp. Nanosci.* **5**, 527 (2010).
- [11] J. Huang, A. X. Lu, B. Zhao, and Q. Wan, *Appl. Phys. Lett.* **91**, 073121 (2007).
- [12] Q. Wan, E. N. Dattoli, and W. Lu, *Appl. Phys. Lett.* **90**, 2221071 (2007).
- [13] A. Espinosa, M. Garcia-Hernandez, N. Menendez, C. Prieto, and A. De-Andres, *Phys. Rev. B* **81**, 064419 (2010).
- [14] W. Prellier, A. Fouchet, and B. Mercey, *J. Phys.: Condens. Matter*. **15**, R1583 (2003).
- [15] R. Long and N. J. English, *Phys. Lett. A* **374**, 319 (2009).
- [16] E. N. Dattoli, Q. Wan, W. Guo, Y. Chen, X. Pan, and W. Lu, *Nano Lett.* **7**, 2463 (2007).
- [17] N. Amin, T. Isaka, A. Yamada, and M. Konagai, *Sol. Energy Mater. Sol. Cells*. **67**, 195 (2001).
- [18] Z. Ying, Q. Wana, H. Cao, Z. T. Song, and S. L. Feng, *Appl. Phys. Lett.* **87**, 1131081 (2005).
- [19] S. Gubbala, V. Chakrapani, V. Kumar, and K. S. Mahendra, *Adv. Funct. Mater.* **18**, 2411 (2008).
- [20] X. Liu, J. Iqbal, Z. Wu, B. He, and R. Yu, *J. Phys. Chem. C* **114**, 4790 (2010).
- [21] A. Maiti, J. A. Rodriguez, M. Law, P. Kung, J. R. McKinney, and P. D. Yang, *Nano Lett.* **3**, 1025 (2003).
- [22] M. Law, H. Kind, B. Messer, F. Kim, and P. D. Yang, *Angew. Chem., Int. Ed.* **41**, 2405 (2002).
- [23] C.-L. Cheng, J.-S. Lin, and Y.-F. Chen, *Mater. Lett.* **62**, 1666 (2008).
- [24] X. H. Ding, D. W. Zeng, and C. S. Xie, *Sens. Actuators. B* **149**, 336 (2010).
- [25] X. F. Liu, J. Iqbal, Z. B. Wu, B. He, and R. H. Yu, *J. Phys. Chem. C* **114**, 4790 (2010).
- [26] I. Saadeddin, H. S. Hilal, B. Pecquenard, J. Marcus, A. Mansouri, C. Labrugere, M. A. Subramanian, and G. Campet, *Sol. Stat. Sci.* **61**, 1060 (2007).
- [27] X. Jia, Y. Liu, X. Wu, and Z. Zhang, *Appl. Surf. Sci.* **311**, 609 (2014).
- [28] S. S. Bhande, D. V. Shinde, S. F. Shaikh, S. B. Ambade, R. B. Ambade, R. S. Mane, Inamuddin, M. Naushad, and S. H. Han, *RSC Advances*. **4**, 20527 (2014).
- [29] S. Yanagiya, N. V. Nong, J. Xu, M. Sonne, and N. Pryds, *J. Electron. Mater.* **40**, 674 (2011).
- [30] H. W. Kim and S. H. Shim, *J. Korean Phys. Soc.* **47**, 516 (2005).
- [31] H. W. Kim, S. H. Shim, and J. W. Lee, *Carbon*. **45**, 2695 (2007).
- [32] T. L. Credelle, C. G. Fonstad, and R. H. Rediker, *Bull. Am. Phys. Soc.* **16**, 519 (1971).
- [33] J. Q. Hu, Y. Bando, Q. Liu, and D. Golberg, *Adv. Funct. Mater.* **13**, 493 (2003).
- [34] B. Cheng, J. M. Russell, W. Shi, L. Zhang, and E. T. Samulski, *J. Am. Chem. Soc.* **126**, 5972 (2004).
- [35] J. Jeong, S.-P. Choi, C. I. Chang, D. C. Shin, J. S. Park, B.-T. Lee, Y.-J. Park, and H.-J. Song, *Solid. Stat. Commun.* **127**, 595 (2003).
- [36] A. K. Mahapatra, U. M. Bhatta, and T. Som, *J.*

- Phys. D: Appl. Phys. **45**, 415303 (2012).
- [37] N. Cabrera and N. F. Mott, Rep. Prog. Phys. **12**, 163 (1949).
- [38] R. Nakamura, J.-G. Lee, D. Tokozakura, H. Mori, and H. Nakajima, Mater. Lett. **61**, 1060 (2007).
- [39] P. P. Sahay, R. K. Mishra, S. N. Pandey, S. Jha, and M. Shamsuddin, Curr. Appl. Phys. **13**, 479 (2013)